IEEE Access
Multidisciplinary | Rapid Review | Open Access Journal

Received July 28, 2019, accepted August 22, 2019, date of publication August 27, 2019, date of current version September 13, 2019.

Digital Object Identifier 10.1109/ACCESS.2019.2937904

Integrated Control With DYC and DSS for 4WID Electric Vehicles

JIE TIAN[1], QUN WANG[1], JIE DING[1], YAQIN WANG[2], AND ZHESHU MA[1]
[1]College of Automobile and Traffic Engineering, Nanjing Forestry University, Nanjing 210037, China
[2]School of Mechanical Engineering, Nanjing University of Science and Technology ZiJin College, Nanjing 210046, China

Corresponding author: Jie Tian (njtianjie@163.com)

This work was supported in part by the National Natural Science Foundations of China under Grant 51975299, Grant 11272159, and Grant 51305207, and in part by the High Level Talent Fund of Nanjing Forestry University under Grant GXL2018004.

ABSTRACT This paper investigates the front-wheel differential steering system (DSS) for a four-wheel independent-drive (4WID) electric vehicle (EV) with a steer-by-wire (SBW) system in case of the steering failure. The nonlinear dynamic model of differential steering vehicle (DSV) is established and the stability regions at different adhesion coefficients are determined based on the theory of phase plane. The traditional front-wheel steering vehicle is selected as the reference model. The direct yaw moment control (DYC) aiming to restore the vehicle to the stability region, and the DSS control aiming to achieve the normal steering function based on the theory of model reference sliding mode control, are researched and applied to the nonlinear dynamic model successively. The direct yaw moment and differential driving torque of the front-wheel needed for the vehicle stability and DSS are obtained respectively. The simulation results show that the proposed integrated control can simultaneously ensure the differential steering and vehicle stability of the nonlinear vehicle on different adhesion coefficient roads.

INDEX TERMS Differential steering system, four-wheel independent-drive, differential steering vehicle, direct yaw moment, integrated control.

I. INTRODUCTION

The appearance of four-wheel independent-drive (4WID) electric vehicles (EV), whose driving motors are mounted into the wheels, enables the independent control of motors, eases the process of vehicle yaw control, and opens up the possibility of differential steering system (DSS) [1]–[5]. Here the DSS refers to the way of realizing steering by controlling the driving moments of the left and right front wheels so that the front steering wheels can rotate around their kingpins at different angles respectively. It differs from the traditional steering system in that the cause of wheel steering is the differential driving moment between the left and right front wheels, rather than the steering wheel. Therefore, the input of steering wheel is just an instruction of the vehicle.

At present, the research on the DSS is very limited, which usually used as the backup system after the failure of steering motor for SBW system, and the non-linear characteristics of tires are not taken into account. However, for the vehicles equipped with the SBW system, the steering of vehicles is driven by the steering motors, but the steering motor may be out of order and unable to turn in the using process, which leads to the failure of SBW.

The dynamic model of the DSS with the failure of steer-by-wire (SBW) was built and a H_∞ controller for the DSS was designed to guarantee the robustness with the consideration of the parametric uncertainty and external disturbances [6]. Aiming to suppress the model uncertainty and road disturbance, a H_∞ mixed sensitivity controller for the DSS was proposed and the simulation results confirmed the efficacy [7]. Compared with the skid steering, the sliding mode variable structure controller for the differential steering of DSV was designed to achieve the normal steering and simulation results proofed the possibility [8]. However, the tire nonlinear characteristic was not taken into account in all of the above researches.

In fact, the DSS cannot only be used as the backup system after the steering failure, but also realize the active steering to greatly improve the vehicle handling stability if the reference model is reasonably selected. However, the DSS can only achieve the normal steering and improve the handling stability when the tires are in the linear region. Because once the tire lateral force is saturated, its normal or active steering ability of DSS can be dramatically reduced,

The associate editor coordinating the review of this article and approving it for publication was György Eigner.

and the vehicle even loses the stability. As another active safety technology, direct yaw moment control (DYC), which gets yaw moment from the differential driving or braking, can restore the vehicle from unstable state to stable one [9]. In summary, the separate control cannot effectively balance the driving safety and handling stability. Therefore, many scholars pay attention to the integrated control, such as the active front or rear steering (AFS/ARS) and DYC, but rarely involve the DYC and DSS.

An integrated vehicle dynamic control (IVDC) algorithm was proposed to improve vehicle handling and stability under critical lateral motions [10]. Reference [11] proposed a nonlinear model predictive controller, which control objective was to track a desired path for obstacle avoidance maneuver by a combined use of the braking and steering. A dynamic control allocation approach was presented for the vehicle yaw stabilization scheme [12]. Based on the steering dynamics segmentation affine model for the tire slip angle and steering angle, a switched model predictive controller was implemented to coordinate the active front steering and differential braking [13]. In reference [14], the researchers proposed a new integrated robust model matching chassis controller to improve vehicle handling performance and lane retention capacity. A controller that integrated the longitudinal force compensation [15], and gain-scheduled linear parameter-varying (LPV) controller [16] were proposed to coordinate the AFS/ARS and DYC to improve the handling and stability for the normal ground vehicles. The 4WID and four-wheel independent-steering (4WIS) systems were coordinated to improve the vehicle driving safety and handling stability according to the ''critical value'' between the yaw rate and vehicle velocity [17].

In this paper, the integrated control with DYC and DSS is proposed for the vehicle equipped with a SBW. Based on the phase plane theory, the stability regions of the nonlinear vehicle model at different adhesion coefficients are confirmed. When the steering motor of SBW fails, the DYC control is firstly carried out to ensure that the vehicle is in the stability region, and then the DSS control based on the sliding mode control is applied to achieve the normal steering.

The rest of this paper is as follows. The differential steering vehicle model including the nonlinear tire model, and the reference model are introduced in Section II. The integrated control strategy of DYC and DSS is presented in Section III. Section IV is the determination of stability regions and design of the DYC controller. The sideslip angle observer and design of the DSS controller are presented in section V. Simulation results are analyzed in Section VI. Section VII is the conclusion.

II. VEHICLE MODELS

In this section, we will first present several models including the linear model of the vehicle equipped with a SBW, nonlinear tire model and reference model. Here the lateral and longitudinal load transfers of the vehicle are neglected, the longitudinal velocity is assumed to be constant, and the left and right tire slip angles are considered to be equal.

A. CONTROL-ORIENTED MODEL FOR VEHICLE WITH DIFFERENTIAL STEERING

For a 4WID EV equipped with a SBW system, the driver's intention is just provided to the electronic control unit (ECU), which will give command to the steering actuator to realize the steering. However, in case of the sudden failure of the steering actuator, we can still steer the vehicle by adjusting the driving torques of the two sides of front wheel, which will make the front wheels rotate around their respective kingpin axes by different angles. That is to say, at this special moment the normal steering function can be realized by the DSS.

The DSS and control-oriented dynamic model of vehicle are shown in Fig. 1, where τ_a is the tire self-aligning moment, r_σ is the scrub radius, F_{xij} and $F_{yij}(i = f, r, j = l, r)$ are the longitudinal and lateral forces of the left/right front/rear wheel, $T_{ij}(i = f, r, j = l, r)$ is the driving torque of left/right front/rear wheel, $l_s$is the half of front wheel track, $l_i(i = f, r)$ is the distance from the center of gravity (CG) to front/rear axle, $k_i(i = f, r)$ is the cornering stiffness of front /rear tire, α_i is the front/rear wheel slip angle, u_x and u_y are the longitudinal and lateral velocities at CG point, β and γ are the sideslip angle and yaw rate of the vehicle, and δ_f is the front-wheel steering angle generated by the differential driving torque.

If the inertia and damping of the steering system are equivalent to the front wheels, the DSS can be simplified to a one-degree-of-freedom second-order system. And the dynamic

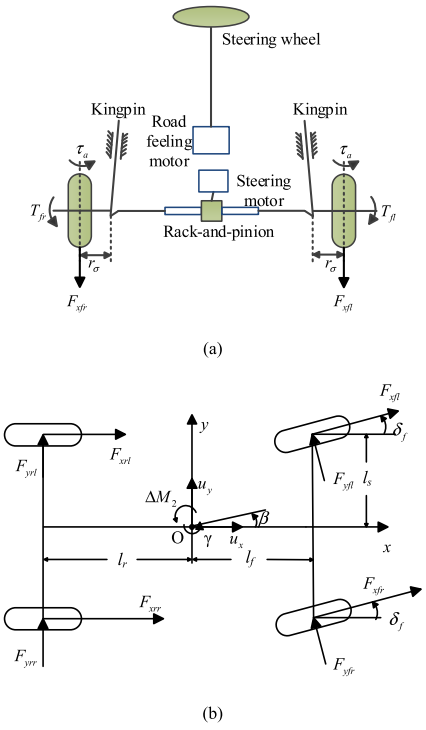

FIGURE 1. Control-oriented vehicle model. (a) Differential steering system of a vehicle with DYC. (b) Dynamic model of a vehicle with DYC.

equation of the DSS as shown in Fig. 1(a) can be expressed as [6]

$$J_e\ddot{\delta}_f + b_e\dot{\delta}_f = \tau_a + \frac{\Delta M_1}{R}r_\sigma - \tau_f$$
$$\tau_a = k_f\alpha_f l^2\Big/3, \quad \alpha_f = \beta + l_f\gamma\big/u_x - \delta_f \tag{1}$$

where J_e and b_e are the effective inertia moment and steering damping of the steering system, ΔM_1 is the differential driving torque between the left and right front wheels, R is the radius of front wheel, α_f is the front wheel slip angle, l is the half of pneumatic trail, τ_f is the friction torque of the steering system, $\ddot{\delta}_f$ and τ_f can be assumed as bounded disturbances.

Ignoring the influence of vehicle suspension, the effects of the aerodynamic force and tire aligning moment, and considering that the vehicle only does plane motion parallel to the ground, that is, the vehicle only has a lateral movement and yaw motion. It is assumed that the driving force is not large, and the influence of ground tangential force on the tire cornering characteristics is not considered. The lateral and yaw motion of a vehicle with DYC (in which roll, pitch and vertical dynamics are neglected), as shown in Fig. 1(b), can be written as

$$\begin{cases} mu_x(\dot{\beta}+\gamma) = \left(F_{yfl}+F_{yfr}\right)\cos\delta_f \\ \qquad\qquad + \left(F_{xfl}+F_{xfr}\right)\sin\delta_f + F_{yrl} + F_{yrr} \\ I_Z\dot{\gamma} = \left(l_f\sin\delta_f + l_s\cos\delta_f\right)\dfrac{\Delta M_1}{R} - l_r(F_{yrl}+F_{yrr}) \\ \qquad\qquad + \left(l_f\cos\delta_f - l_s\sin\delta_f\right)(F_{yfl}+F_{yfr}) + \Delta M_2 \end{cases} \tag{2}$$

where m is the total vehicle mass, I_z is the yaw moment of inertia, ΔM_2 is the yaw moment generated by the longitudinal tire forces of the rear wheels, as shown in Fig. 1(b).

For analytical considerations the motion equations for the vehicle are linearized, i.e. only small angles with $\sin\alpha_f \approx \alpha_f$ and $\cos\alpha_f \approx 1$ are considered and a linear tire behavior is assumed, then

$$\begin{cases} F_{yfl} = F_{yfr} = k_f\left(\beta + l_f\gamma\big/u_x - \delta_f\right) \\ F_{yrl} = F_{yrr} = k_r\left(\beta - l_r\gamma\big/u_x\right) \end{cases} \tag{3}$$

Assume $\Delta M_2 = 0$, and define $X(t) = \left[\beta \;\; \gamma \;\; \delta_f\right]^T$, $U(t) = \Delta M_1$, (1) - (3) can be rewritten as

$$\dot{X} = A_sX + B_sU$$
$$A_s = \begin{bmatrix} \dfrac{2k_f+2k_r}{mu_x} & \dfrac{2k_fl_f-2k_rl_r}{mu_x^2} - 1 & \dfrac{2k_f}{mu_x} \\ \dfrac{2k_fl_f-2k_rl_r}{I_Z} & \dfrac{2k_fl_f^2+2k_rl_r^2}{I_Zu_x} & -\dfrac{2k_fl_f}{I_Z} \\ \dfrac{k_fl^2}{3b_e} & \dfrac{k_fl^2l_f}{3b_eu_x} & -\dfrac{k_fl^2}{3b_e} \end{bmatrix},$$
$$B_s = \begin{pmatrix} 0 \\ \dfrac{l_s}{I_ZR} \\ \dfrac{r_\sigma}{Rb_e} \end{pmatrix} \tag{4}$$

However, when we consider the tire nonlinearity, F_{yij} can be described as the following according to the Pacejka tire model [18].

$$\begin{cases} F_{yfl} = F_{yfr} = \mu F_{zf}\sin[D_f\text{arc an}(B_f\alpha_f)] \\ F_{yrl} = F_{yrr} = \mu F_{zr}\sin[D_r\text{arc an}(B_r\alpha_r)] \end{cases} \tag{5}$$

where μ is the road adhesion coefficient, $F_{zi}(i = f, r)$ is the vertical load of the front/rear wheel, B_i and $D_i(i = f, r)$ are the fitting coefficients.

And the nonlinear tire model of vehicle, which will be used in the simulation, can be achieved by substituting (5) into (2). Here the tire lateral force and its fitting results when $\mu = 1$ are shown in Fig. 2. By giving the initial value of B_i and D_i, and adjusting them repeatedly according to the difference between the fitting curve and actual curve, $B_i = 0.325$, $D_i = 1.535$ are obtained.

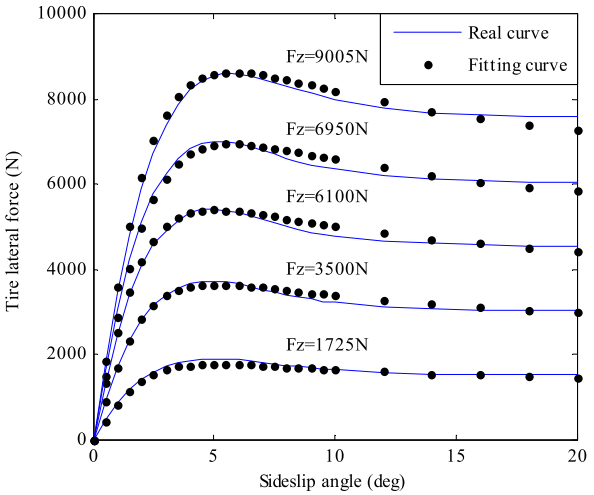

FIGURE 2. Tire lateral force at different vertical loads.

B. B.REFERENCE MODEL

Here the single track vehicle model is taken as the reference model, which is used to obtain the reference sideslip angle and yaw rate according to the input of front-wheel steering angle proportional to the steering angle commanded by driver.

Define $x_d(t) = \left[\beta_d \;\; \gamma_d\right]^T$ and $u_d(t) = \delta$, then the reference model can be modeled as

$$\begin{cases} \dot{x}_d = A_dx_d + B_du_d \\ y_d = C_dx_d \end{cases}$$
$$A_d = \begin{pmatrix} \dfrac{2(k_f+k_r)}{mu_x} & -1 + \dfrac{2l_{fd}k_f - 2l_{rd}k_r}{mu_x^2} \\ \dfrac{2l_{fd}k_f - 2l_{rd}k_r}{I_Z} & \dfrac{2l_{fd}^2k_f + 2l_{rd}^2k_r}{I_zu_x} \end{pmatrix},$$
$$B_d = \begin{pmatrix} \dfrac{2k_f}{mu_x} \\ \dfrac{2l_{fd}k_f}{I_Z} \end{pmatrix}, \quad C_d = \begin{pmatrix} 1 & 0 \\ 0 & 1 \end{pmatrix} \tag{6}$$

where δ is the front-wheel steering angle generated by the steering wheel commanded by the driver, β_d, γ_d, and $l_{id}(i = f, r)$ are the sideslip angle, yaw rate, distance from CG to front/rear axle of the reference model respectively.

III. PROBLEM FORMULATION

Usually the input of reference model is the front-wheel steering angle. While for the vehicle with the failure of the steering motor, the input is the differential driving torque between the two sides of front driving wheels. When the tire nonlinearity is not considered, the DSS control based on the sliding mode variable structure theory can completely make the vehicle obtain the normal steering in case of the SBW failure [8]. However, when the sideslip angle of tire becomes large, the tire will present the nonlinear characteristic, the lateral force acting on the tire will tend to be saturated and the road cannot provide the sufficient lateral force. At this time, the DSS control effect is not ideal. However, the DYC control effect, which can adjust the yaw motion and improve the vehicle stability by distributing the braking or driving force on wheels, is very good. Therefore, the integrated control of DYC and DSS, as shown in Fig. 3, is proposed to ensure that the yaw rate of the nonlinear vehicle can follow their reference one calculated by (6).

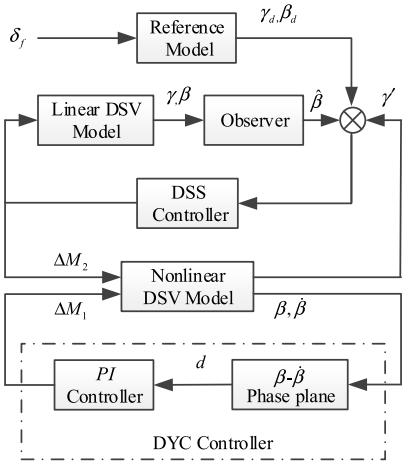

FIGURE 3. Control block diagram of integrated controller.

In addition, the steering motor is equipped with an angle sensor. When the steering motor works normally, there is a certain correlation between the steering angle of the steering motor and that of the steering wheel. When the driver rotates the steering wheel, the electronic control unit (ECU) cannot collect the signal of the steering motor angle sensor for a certain time after collecting the steering wheel angle signal, or the signal is always close to 0, or far from matching the collected signal of the steering wheel angle, the ECU will determine the failure of the steering motor, and then enter the DSS steering control mode.

As shown in Fig. 3, the DSS controller is firstly designed according to the reference model and linear vehicle. Then the closed-loop control of the non-linear vehicle by the DSS controller is carried out, and the phase plane is drawn at the same time. When the phase trajectory exceeds the stability region of the phase plane, i.e., the distance from the unstable phase point to the boundary of stability region is larger than 0 (i.e., $d > 0$), the DYC controller will act to restore the vehicle back to the stability region, and the needed yaw moment, ΔM_2, which will be achieved applying different longitudinal forces to left and right rear wheels. And at this time, the vehicle state is close to the equilibrium point in normal driving conditions (low accelerations) and the nonlinear vehicle is close to a linear one, so the differential steering can be completely achieved by the DSS controller on the basis of the DYC controller. And the differential driving torque of the front wheels, ΔM_1, can be got. Under the combined action of these two kinds of torques, the DSV vehicle can achieve the same steering characteristics as the reference model. While when the phase trajectory is always inside of the stability region, the output of the DYC controller will be 0. That is to say, it is the combination of the DSS and DYC controllers that ensure the nonlinear vehicle to achieve the normal steering on different adhesion coefficient roads.

IV. DESIGN OF DYC CONTROLLER

Based on the phase plane theory, DYC controller will be designed to control the stability of non-linear vehicles. The main purpose is to make the phase trajectory inside of the stability region and recovery the vehicle from an unstable state to a stable one. Therefore, it is necessary to ascertain the stability region, in which the nonlinear vehicle is close to a linear one.

A. DETERMINATION OF STABILITY REGION

As we all known, there are two types of phase plane for vehicle [19]: $\beta - \gamma$ and $\beta - \dot{\beta}$. Related studies show that the latter can reflect the vehicle stability more accurately [20]. And here we establish the stability region by the latter. Setting $\Delta M_2 = 0$Nm and giving different initial values (β (0), γ (0)), the $\beta - \dot{\beta}$ phase planes with $\mu = 0.2$ and $u_x = 10$m/s, and $\mu = 0.8$ and $u_x = 33.3$m/s are obtained, as shown in Fig. 4.

It can be seen from Fig. 4 that both of the phase trajectories can eventually converge to the phase point (0,0) and two parallel lines can be drawn to include the trajectories that can return to the phase point (0,0). Their stability regions surrounded by the two symmetrical virtual lines in Fig. 4 can be described as [19]

$$\left|B_1\dot{\beta} + \beta\right| \le B_2 \tag{7}$$

where B_1 and B_2 are the boundary coefficients of stability region.

The vehicle state out of the region is unstable. However, when the state is inside the stability region, the phase trajectory lines started from any initial value will converge to the origin. And only when (7) holds, the vehicle can be regarded as linear, or vice versa. The parameters of (7) can be calculated by reading the coordinates of any two points on the line and the boundaries, shown in Fig. 4(a) and 4(b), can be expressed as

$$\begin{cases} \left|3.0303\dot{\beta} + \beta\right| = 0.053 & (\mu = 0.2) \\ \left|7.2581\dot{\beta} + \beta\right| = 9.032 & (\mu = 0.8) \end{cases} \tag{8}$$

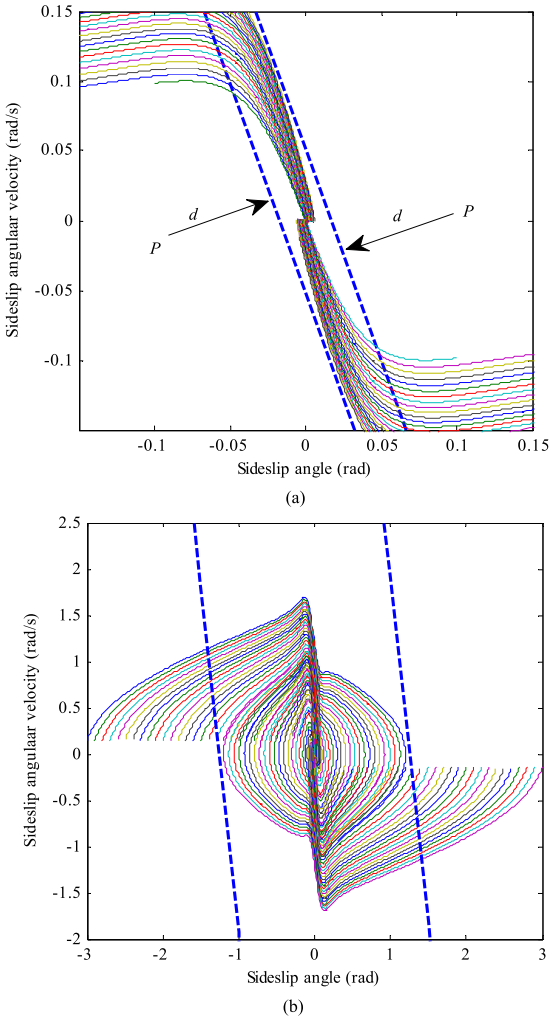

FIGURE 4. Phase plane. (a) $\mu = 0.2$, $u_x = 10$m/s and $\Delta M_2 = 0$Nm. (b) $\mu = 0.8$, $u_x = 33.3$m/s and $\Delta M_2 = 0$Nm.

B. PI CONTROLLER OF DYC

Assume that the status point, P, is out of the stability region, the distance from the unstable phase point to the boundary of stability region is d (as shown in Fig. 4(a)). And d can be expressed as

$$d(t) = \begin{cases} \dfrac{|B_1\dot{\beta}_0 + \beta_0 - B_2|}{\sqrt{B_1^2 + 1}} & (P \text{ is above the region}) \\ \dfrac{|B_1\dot{\beta}_0 + \beta_0 + B_2|}{\sqrt{B_1^2 + 1}} & (P \text{ is below the region}) \end{cases} \tag{9}$$

The purpose of DYC is to recovery the vehicle from an unstable state to a stable one, i.e., to make d be zero. Here a proportional and integral controller (shown in Fig. 3), whose input and output are $d(t)$ and ΔM_2, is adopted to make d be zero. And

$$\Delta M_2(t) = K_p d(t) + \frac{K_I}{T_i}\int_0^t d(t)dt \tag{10}$$

where K_p and K_I are the proportional and integral coefficients. And these two parameters are adjusted by returning the phase trajectory to the stability region.

First, K_I is removed to make it a pure proportional regulation. The proportional coefficient increases gradually from 0 until the system oscillates; on the other hand, K_p decreases gradually from this time until the system oscillates slightly. Record the proportional coefficient at this time. After that, a large K_I is set, then it decreases gradually until the system oscillates, and then increases gradually until the system oscillations disappear. Finally, K_p and K_I are fine-tuned until the performance requirements are met.

V. DESIGN OF DSS CONTROLLE

The purpose of DSS controller is to achieve the normal steering by the differential driving torque of the front wheels. As shown in Fig. 3, the input of reference model is the front-wheel steering angle. According to the reference model, the DSS controller can generate a differential driving torque to achieve the normal steering for vehicles whose steering system fails. However, the sensors to measure the sideslip angle usually are very expensive [21], therefore the observer should be designed to estimate the actual sideslip angle.

A. SIDESLIP ANGLE OBSERVER

Define $\bar{X}_1 = [\beta]$, $\bar{X}_2 = \begin{bmatrix} \gamma & \delta_f \end{bmatrix}$, (4) can be expressed as

$$\begin{cases} \begin{bmatrix} \dot{\bar{X}}_1 \\ \dot{\bar{X}}_2 \end{bmatrix} = \begin{bmatrix} \bar{A}_{11} & \bar{A}_{12} \\ \bar{A}_{21} & \bar{A}_{22} \end{bmatrix} \begin{bmatrix} \bar{X}_1 \\ \bar{X}_2 \end{bmatrix} + \begin{bmatrix} \bar{B}_1 \\ \bar{B}_2 \end{bmatrix} U \\ \bar{Y} = \begin{bmatrix} 0 & I \end{bmatrix} \begin{bmatrix} \bar{X}_1 \\ \bar{X}_2 \end{bmatrix} = \bar{X}_2 \end{cases}$$

$$\bar{A}_{11} = \left[\frac{2k_f + 2k_r}{mu_x}\right],$$

$$\bar{A}_{12} = \left[\frac{2k_f l_f - 2k_r l_r}{mu_x^2} - 1 \quad \frac{2k_f}{mu_x}\right],$$

$$\bar{A}_{21} = \begin{bmatrix} \dfrac{2k_f l_f - 2k_r l_r}{I_Z} & \dfrac{2k_f l_f^2 - 2k_r l_r^2}{I_Z u_x} \\ \dfrac{k_f l^2}{3b_e} & \dfrac{k_f l^2 l_f}{3b_e u_x} \end{bmatrix},$$

$$\bar{A}_{22} = \begin{bmatrix} -\dfrac{2k_f l_f}{I_Z} \\ -\dfrac{k_f l^2}{3b_e} \end{bmatrix},$$

$$\bar{B}_1 = [0], \quad \bar{B}_2 = \begin{bmatrix} \dfrac{l_s}{I_Z R} \\ \dfrac{r_\sigma}{R b_e} \end{bmatrix} \tag{11}$$

And (11) can be rewritten as

$$\begin{cases} \dot{\bar{X}}_1 = \bar{A}_{11}\bar{X}_1 + \bar{A}_{12}\bar{Y} + \bar{B}_1 U \\ Z = \bar{A}_{21}\bar{X}_1 \end{cases} \tag{12}$$

where

$$Z = \dot{\bar{Y}} - \bar{A}_{22}\bar{Y} - \bar{B}_2 U \tag{13}$$

The observer dynamic equation can be defined as,

$$\begin{cases} \dot{\hat{X}}_1 = \bar{A}_{11}\hat{X}_1 + \bar{A}_{12}\bar{Y} + \bar{B}_1 U - H\left(\hat{Z} - Z\right) \\ \hat{Z} = \bar{A}_{21}\hat{X}_1 \end{cases} \tag{14}$$

Substituting (13) into (14), the following can be obtained.

$$\dot{\hat{X}}_1 = \left(\bar{A}_{11} - H\bar{A}_{21}\right)\hat{X}_1 + \left(\bar{A}_{12}\bar{Y} + \bar{B}_1 U\right) + H\left(\dot{\bar{Y}} - \bar{A}_{22}\bar{Y} - \bar{B}_2 U\right) \tag{15}$$

where $\left(\bar{A}_{11} - H\bar{A}_{21}\right)$ is the coefficient matrix. And the poles of reduced-order observer can be determined by the following characteristic equation.

$$\left|\lambda I - \left(\bar{A}_{11} - H\bar{A}_{21}\right)\right| = 0 \tag{16}$$

Define

$$W = \hat{X}_1 - H\bar{Y} \tag{17}$$

then

$$\dot{\hat{X}}_1 = \dot{W} + H\dot{\bar{Y}} = \left(\bar{A}_{11} - H\bar{A}_{21}\right)\left(W + H\bar{Y}\right) + \left(\bar{A}_{12}\bar{Y} - \bar{B}_1 U\right) + H\dot{\bar{Y}} - H\bar{A}_{22}\bar{Y} - H\bar{B}_2 U \tag{18}$$

And the following can be obtained

$$\begin{cases} \hat{X}_1 = W + H\bar{Y} \\ \dot{W} = \left(\bar{A}_{11} - H\bar{A}_{21}\right)W + \left(\bar{B}_1 - H\bar{B}_2\right)U \\ \qquad + \left[\left(\bar{A}_{11} - H\bar{A}_{21}\right)H + \bar{A}_{12} - H\bar{A}_{22}\right]\bar{Y} \end{cases} \tag{19}$$

Subtracting (15) from (12), and

$$\dot{\bar{X}}_1 - \dot{\hat{X}}_1 = \left(\bar{A}_{11} - H\bar{A}_{21}\right)\left(\bar{X}_1 - \hat{X}_1\right) \tag{20}$$

Because (20) is homogeneous, its poles can be disposed arbitrarily [22] as long as H is selected correctly. And the satisfactory decay rate of $\left(\bar{X}_1 - \hat{X}_1\right)$can be achieved and $\hat{X}_1$can approach $\bar{X}_1$ as soon as possible.

B. SLIDING MODE CONTROLLER OF DSS

Define its sliding surface as

$$s = \gamma - \gamma_d + \xi\left(\hat{\beta} - \beta_d\right) \tag{21}$$

where ξ is the weight coefficient.

Take the derivative of (21) and substitute (2) and (19) into (21), the following equation can be obtained.

$$\begin{aligned} \dot{s} &= d_1 + d_2 + \frac{l_s}{I_Z R}\Delta M_1 + D_1(t) \\ d_1 &= -\frac{2k_f l_f}{I_Z}\delta_f + \frac{2k_f l_f - 2k_r l_r}{I_Z}\beta + \frac{2k_f l_f^2 - 2k_r l_r^2}{I_Z u_x}\gamma \\ d_2 &= \xi\left[\frac{2k_f}{mu_x}\delta_f + \frac{2k_f + 2k_r}{mu_x}\beta + \left(\frac{2k_f l_f - 2k_r l_r}{mu_x^2} - 1\right)\gamma\right], \\ D_1(t) &= -\left[\dot{\gamma}_d + \xi\dot{\beta}_d - \xi(\bar{A}_{11} - H\bar{A}_{21})\left(\beta - \hat{\beta}\right)\right] \end{aligned} \tag{22}$$

Because of the convergent of the sideslip angle observer, $\beta - \hat{\beta}$ will converge to zero in a finite time. And it can be drawn from (2) that $\dot{\gamma}_d$ and $\dot{\beta}_d$ are bounded. Then the following holds.

$$|D_1(t)| \le \bar{D}_1 \tag{23}$$

where $\bar{D}_1$ is a constant.

Here the exponential reaching law with saturation function is adopted to reduce the chattering phenomenon, and the controller can be designed as

$$\Delta M_1 = \frac{I_Z R}{l_s}\left[-k_1 \mathrm{sat}(s) - k_2 s - d_1 - d_2\right] \tag{24}$$

where $k_1 > \bar{D}_1, k_2 > 0$.

Substitute (24) into (22), then

$$\dot{s} = \frac{1}{I_Z}\left[-k_1 \mathrm{sat}(s) - k_2 s + D_1(t)\right] \tag{25}$$

Define Lyapunov function as

$$V(s) = \frac{1}{2}s^2 \tag{26}$$

Derivate (26) and the following can be got

$$\begin{aligned} \dot{V} &= \frac{1}{I_Z}\left[-k_1 \mathrm{sat}(s) - k_2 s + D_1(t)\right]s \\ &\le \frac{1}{I_Z}\left(-k_1 + \bar{D}_1\right)|s| \end{aligned} \tag{27}$$

Because of $k_1 > \bar{D}_1$, and we can get

$$\dot{V} < \sqrt{2}\frac{k_1 - \bar{D}_1}{I_Z}V^{\frac{1}{2}} \tag{28}$$

According to the Lyapunov stability theory in finite time, s will converge to the origin in a finite time.

VI. SIMULATION RESULTS AND ANALYSIS

In this section, the simulations of double lane change (DLC) are carried out by Simulink/MATLAB for the reference model and nonlinear vehicles with different controller. In Carsim, we select the B-Class Hatchback model, set the simulation conditions, such as the driver's target speed, DLC working condition, simulation time, output variable—steering angle of the steering wheel and simulation step, run the math model, output and save the steering angle data of steering wheel in txt format, which can be imported to and used in Simulink/MATLAB. And according to B-Class Hatchback model, we can get specific vehicle simulation parameters.

This paper mainly studies the feasibility of differential steering after the failure of SBW system, so two kinds of normal working conditions are selected to simulate. The parameters of the B-Class hatchback model used in the simulation are as follows: $m = 1250$kg, $I_z = 2031.4$kgm^2, $l_f = 1.04$m, $l_r = 1.56$m, $l_{fd} = 1.04$m, $l_{rd} = 1.56$m, $l_s = 0.7405$m, $R = 0.304$m.

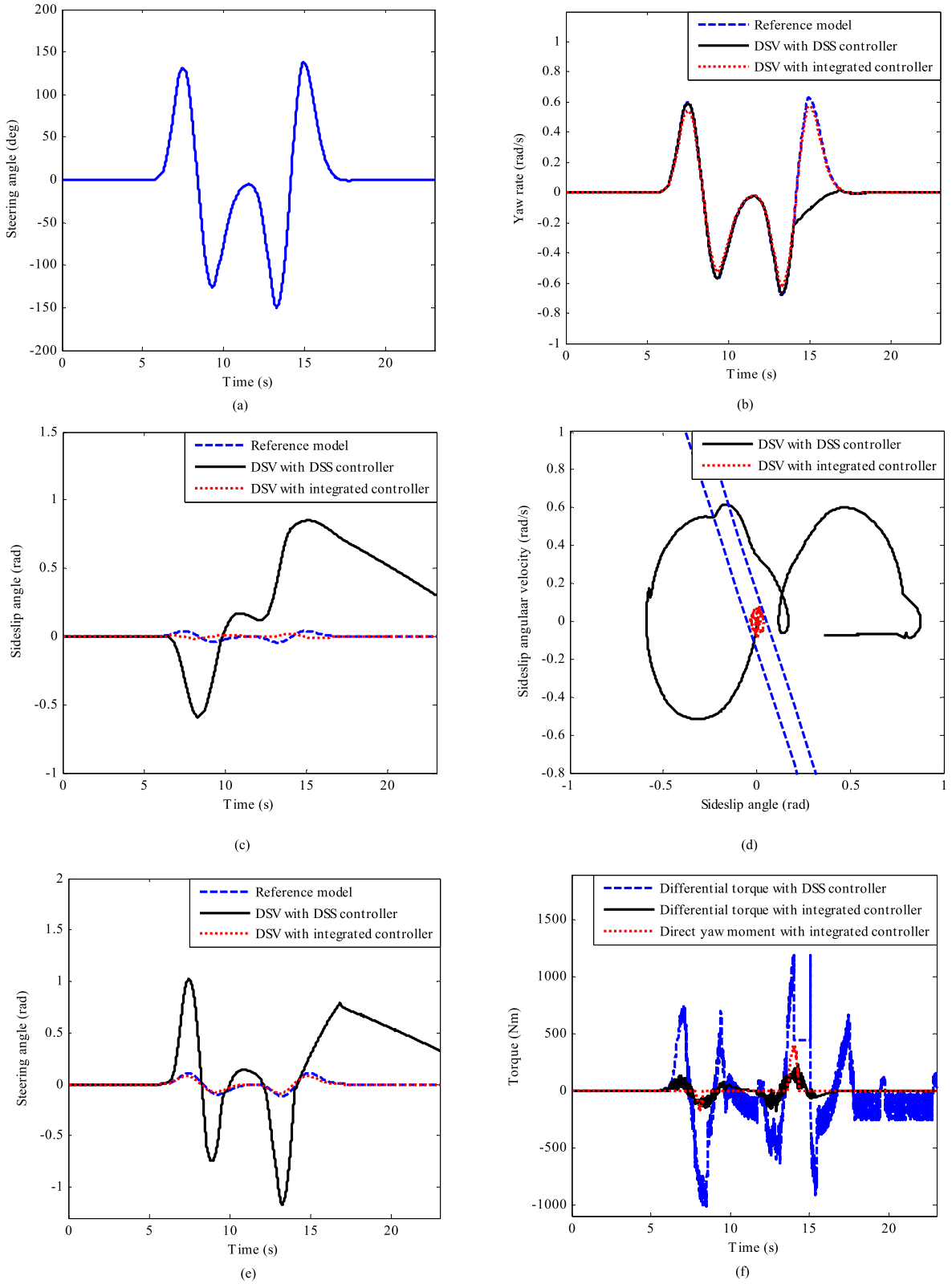

FIGURE 5. Double lane change simulation ($\mu = 0.2$). (a) Steering angle of steering wheel. (b) Sideslip angle curves. (c) Yaw rate curves. (d) Phase plane. (e) Front-wheel steering angles. (f) Torques for DSS and DYC controllers.

A. SIMULATION ON LOW μ ROAD

Here the reference model runs on a low adhesion coefficient road at the speed of 10m/s and its input is shown in Fig. 5(a). At this time, $\mu = 0.2$, $u_x = 10$m/s, $k_f = -20493$N/rad, $k_r = -13617$N/rad, $|\Delta M_1| \leq \mu F_z R = 446.88Nm$, $K_p = 50$ and $K_I = -0.001$. And the simulation

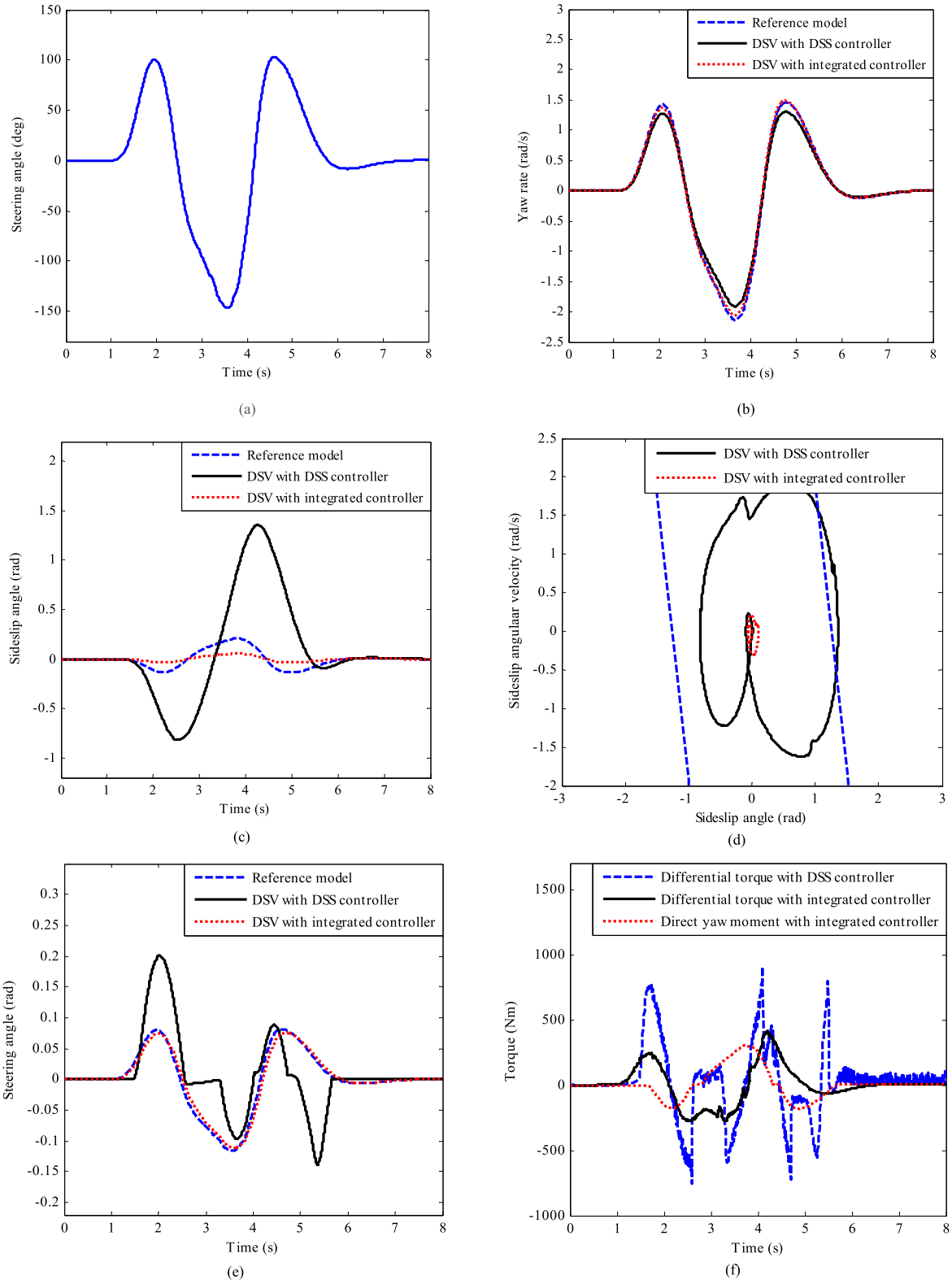

FIGURE 6. Double lane change simulation ($\mu = 0.8$). (a) Steering angle of steering wheel. (b) Yaw rate curves. (c) Sideslip angle curves. (d) Phase plane. (e) Front-wheel steering angles. (f) Torques for DSS and DYC controllers.

results of the reference model, vehicle with DSS controller, and vehicle with integrated controller are illustrated in Fig. 5.

The yaw rates and sideslip angles of the reference model, vehicle with DSS controller, and vehicle with integrated controller are shown in Figs. 5(b) and 5(c). It can be drawn from

Fig. 5(b) that the yaw rate of the vehicle with integrated controller track the reference ones very well, while that of the vehicle with DSS controller are very different from the reference ones after 12.6s. From Fig. 5(c) it can be seen that the absolute maximum of the sideslip angle of the vehicle with DSS controller is 0.8rad, so different with that of the reference model. The reason is that the tire longitudinal force is saturated. However, the sideslip angle of the vehicle with integrated controller is closed to that of the reference model, and the difference between them is mainly due to the intervention of DYC.

The phase planes of the two vehicles are illustrated in Fig. 5(d). It can be seen that most parts of the phase trajectory of the vehicle with DSS controller are out of the stability region while that of the vehicle with integrated controller are all in the region. Therefore, the DYC controller plays a very important role in restoring the vehicle to the stability region.

The input of the reference model and the extra front-wheel steering angles generated by the differential driving torques of the vehicles with different controllers are shown in Fig. 5(e). It presents that the extra front-wheel steering angles of the vehicle with DSS controller is very different from the vehicle with integrated controller. And the extra front-wheel steering angle of the vehicle with integrated controller is almost the same as the steering angle of the reference model.

Fig. 5(f) shows that the absolute maximums of the differential driving torque needed for the vehicle with DSS controller, the differential driving torque and direct yaw moment required for the vehicle with integrated controller are 1120Nm, 240Nm, and 412Nm. The differential torque with DSS controller is not enough to ensure the response of the vehicle to that of the reference model because the tire longitudinal force is saturated and $|\Delta M_1| \leq \mu F_z R = 446.88Nm$. However, the differential torque with the integrated controller is smaller than the limitation of ΔM_1 because of the intervention of DYC. It demonstrates that the intervention of DYC controller significantly reduces the differential driving torques needed for the vehicle with DSS controller

In conclusion, on a low μ road it is necessary for the DYC controller to restore the vehicle to the stability region because the only DSS controller cannot work very well. And the proposed integrated controller is effective for the nonlinear vehicle running on a low μ road to achieve the normal steering in case of the failure of SBW system.

B. SIMULATION ON HIGH μ ROAD

In this maneuver, we define that the reference model moves on a high adhesion coefficient road at the speed of 33.3m/s and its input is shown in Fig. 6(a). At this time, $\mu = 0.8$, $u_x = 33.3$m/s, $k_f = -81694$N/rad, $k_r = -53379$N/rad, $|\Delta M_1| \leq \mu F_z R = 1787.52Nm$, $K_p = 500$ and $K_I = -0.001$. And the simulation results of the reference model, vehicle with DSS controller, and vehicle with integrated controller are illustrated in Fig. 6.

Figs. 6(b) and 6(c) are the yaw rates and sideslip angles of the reference model, vehicle with DSS controller, and vehicle with integrated controller, which show that the yaw rates of the vehicles with DSS controller and integrated controller are almost the same as those of the reference model, but the sideslip angle of the vehicle with DSS controller is so different from that of the reference model. And it can be drawn that at this time the DSS controller cannot ensure the steering of the non-linear vehicle exactly the same as the reference model.

Fig. 6(d) shows the phase planes of the two vehicles, which can be drawn that a little parts of the phase trajectory of the vehicle with DSS controller are out of the stability region, while all parts of the phase trajectory of vehicle with integrated controller are inside of the stability region. And all of the above demonstrate that the integrated controller can effectively guarantee the vehicle stability while achieving the normal steering.

Fig. 6(e) presents the front-wheel steering angle of the reference model and the extra front-wheel steering angles generated by the differential driving torque between the two sides of the front wheels calculated by the two controllers. It can be seen that the additional front-wheel steering angle produced by the vehicle with integrated controller is almost identical to input of the reference model, but that produced by the vehicle with DSS controller is about 2 more times of that of the reference model.

The differential driving torques needed for the vehicle with DSS controller, the differential driving torque and direct yaw moment required for the vehicle with integrated controller are shown in Fig. 6(f), and their absolute maximums are 900Nm, 411Nm and 300Nm, which indicate that the DYC controller does work because sometimes the nonlinear vehicle with DSS controller is out of the stability region as shown in Fig. 6(d).

In summary, even on a high μ road the integrated control is still needed to ensure the good tracking and vehicle stability when the vehicle is out of the stability region.

VII. CONCLUSION

Assuming that the steering motor cannot turn properly and the driver's instructions cannot be responded to, the integrated control of the nonlinear vehicle is studied:

1) Simulation results indicate that the integrated control can ensure the nonlinear vehicle to achieve the normal steering on both high and low μ road while the steering motor fails.
2) When the vehicle is in the stability region, the DSS control is adopted to achieve the normal steering. However, when the vehicle is out of the region, the DYC control will be adopted firstly to restore the vehicle to the region.
3) While the vehicle out of the region, it is the two torques produced by the DYC and DSS controller that guarantees the stability of the vehicle and achieves the differential steering at the same time.

4) The structure of DSS for the vehicle is very simple. It can be used not only as a standby steering system, but also as an active steering system of front and rear wheels to improve vehicle handling stability, and even as the only steering system for the future driverless vehicles.

REFERENCES

[1] B. Leng, L. Xiong, C. Jin, J. Liu, and Z. Yu, "Differential drive assisted steering control for an in-wheel motor electric vehicle," *SAE Int. J. Passenger Cars-Electron. Elect. Syst.*, vol. 8, no. 2, pp. 433–441, Jan. 2015.
[2] C. Y. Sun, X. Zhang, L. Xi, and Y. Tian, "Design of a path-tracking steering controller for autonomous vehicles," *Energies*, vol. 11, no. 6, pp. 1–17, Jan. 2018.
[3] C. N. To, D. V. Quôc, M. Simic, H. Khayyam, and R. N. Jazar, "Autodriver autonomous vehicles control strategy," *Procedia Comput. Sci.*, vol. 126, pp. 870–877, Aug. 2018.
[4] W. Zhao, X. Xu, and C. Wang, "Multidiscipline collaborative optimization of differential steering system of electric vehicle with motorized wheels," *Sci. China-Technol. Sci.*, vol. 55, no. 12, pp. 3462–3468, Dec. 2012.
[5] X. Zhang and D. Göhlich, "Integrated traction control strategy for distributed drive electric vehicles with improvement of economy and longitudinal driving stability," *Energies*, vol. 10, no. 1, p. 126, 2017.
[6] R. R. Wang, H. Jing, C. Hu, M. Chadli, and F. J. Yan, "Robust H∞ output-feedback yaw control for in-wheel motor driven electric vehicles with differential steering," *Neurocomputing*, vol. 173, pp. 676–684, Jan. 2016.
[7] W. Z. Zhao, Y. J. Li, C. Y. Wang, Z. Q. Zhang, and C. L. Xu, "Research on control strategy for differential steering system based on H mixed sensitivity," *Int. J. Automot. Technol.*, vol. 14, no. 6, pp. 913–919, Dec. 2013.
[8] J. Tian, J. Tong, and S. Luo, "Differential steering control of four-wheel independent-drive electric vehicles," *Energies*, vol. 11, no. 11, pp. 1–18, Nov. 2018.
[9] J. Chen, "A novel pre-control method of vehicle dynamics stability based on critical stable velocity during transient steering maneuvering," *Chin. J. Mech. Eng.*, vol. 29, no. 3, pp. 475–485, 2016.
[10] E. Mousavinejad, Q.-L. Han, F. Yang, Y. Zhu, and L. Vlacic, "Integrated control of ground vehicles dynamics via advanced terminal sliding mode control," *Vehicle Syst. Dyn.*, vol. 55, no. 2, pp. 268–294, 2017.
[11] P. Falcone, H. E. Tseng, F. Borrelli, J. Asgari, and D. Hrovat, "MPC-based yaw and lateral stabilisation via active front steering and braking," *Veh. Syst. Dyn.*, vol. 46, no. S1, pp. 611–628, 2008.
[12] J. Tjónnás and T. A. Johansen, "Stabilization of automotive vehicles using active steering and adaptive brake control allocation," *IEEE Trans. Control Syst. Technol.*, vol. 18, no. 3, pp. 545–558, May 2010.
[13] S. D. Cairano and H. E. Tseng, "Driver-assist steering by active front steering and differential braking: Design, implementation and experimental evaluation of a switched model predictive control approach," in *Proc. 49th IEEE Conf. Decision Control (CDC)*, Dec. 2010, pp. 2886–2891.
[14] J. Wu, Q. Wang, X. Wei, and H. Tang, "Studies on improving vehicle handling and lane keeping performance of closed-loop driver-vehicle system with integrated chassis control," *Math. Comput. Simul.*, vol. 80, no. 12, pp. 2297–2308, 2010.
[15] M. Doumiati, O. Sename, L. Dugard, J. J. Martinez-Molina, P. Gaspar, and Z. Szabo, "Integrated vehicle dynamics control via coordination of active front steering and rear braking," *Eur. J. Control*, vol. 19, no. 2, pp. 121–143, 2013.
[16] S. C. Baslamisli, E. Köse, and G. Anlaş, "Gain-scheduled integrated active steering and differential control for vehicle handling improvement," *Veh. Syst. Dyn.*, vol. 47, no. 1, pp. 99–119, 2009.
[17] L. Jin, "Research on the control and coordination of four-wheel independent-driving four-wheel independent-steering electric vehicle," *Adv. Mech. Eng.*, vol. 9, no. 3, pp. 1–13, 2017.
[18] H. B. Pacejka, *Tire and Vehicle Dynamics*. Oxford, U.K.: Butterworth–Heinemann, 2002, pp. 46–50.
[19] M. A. Selby, "Intelligent vehicle motion control," Ph.D. dissertation, Dept. Mech. Eng., Univ. Leeds, Leeds, U.K, 2003.
[20] S. Inagaki, I. Kushiro, and M. Yamamoto, "Analysis on vehicle stability in critical cornering using phase-plane method," *JSAE Rev.*, vol. 2, no. 16, p. 216, 1995.
[21] Y. Zhang, A. Wang, and H. Zuo, "Roller bearing performance degradation assessment based on fusion of multiple features of electrostatic sensors," *Sensors*, vol. 19, no. 4, p. 824, 2019.
[22] H. W. Xie, F. X. Zou, M. Zhang, P. B. Li, and Q. Li, *Morden Control Systems*. 8th ed. Beijing, China: Higher Edu. Press, 2006, pp. 201–204.

JIE TIAN received the B.S. degree in mechanical engineering and automobile engineering and the M.S. degree in mechanics from the Wuhan University of Technology, Wuhan, China, in 1995 and 1998, respectively, the Ph.D. degree in vehicle engineering from Jiangsu University, in 2011, and the postdoctoral degree in mechanical engineering from Nanjing Forestry University, Nanjing, China, in 2017. From 2015 to 2016, she was a Senior Visiting Scholar of Texas Tech University, USA. She is currently an Associate Professor with Nanjing Forestry University. Her current research interests include the vehicle system dynamics and control, and vehicle design CAD/CAE.

QUN WANG received the B.S. degree in vehicle engineering from Nanjing Forestry University, Nanjing, China, in 2017, where she is currently pursuing the M.S. degree in vehicle engineering with the Department of Traffic and Transportation. Her research interests include electric vehicle active safety and electric vehicle stability control systems.

JIE DING received the B.S. degree in vehicle engineering from Nanjing Forestry University, Nanjing, China, in 2018, where she is currently pursuing the M.S. degree in vehicle engineering with the Department of Traffic and Transportation. Her research interest includes the vehicle system dynamics and control.

YAQIN WANG received the B.S. degree in machinery manufacturing and automation and the M.S. degree in transportation engineering from Nanjing Forestry University, Nanjing, China, in 2006 and 2012, respectively. She is currently a Lecturer with the Department of Vehicle Engineering, College of Mechanical Engineering, Nanjing University of Science and Technology Zijin College. Her current research interest includes the vehicle system dynamics and control.

ZHESHU MA received the B.S. and M.S. degrees in energy and power engineering from the Jiangsu University of Science and Technology, Jiangsu, China, in 1996 and 1999, respectively, and the Ph.D. degree in man–machine and environmental engineering from the Nanjing University of Aeronautics and Astronautics, Jiangsu, in 2004. From 2008 to 2009 and from 2014 to 2015, he was a Senior Visiting Scholar of The University of Manchester, U.K., and the University of Virginia, USA, respectively. He is currently a Full Professor with Nanjing Forestry University, Jiangsu. His current research interests include the new energy vehicle technology and advanced thermal management.